Electronic Supplementary Material (ESI) for Soft Matter.

Supplementary Material

A Microstructural Investigation of an Industrial Attractive Gel at Pressure and Temperature

Andrew Clarke[†,a], Elizabeth Jamie[a], Nikolaos A. Burger[b], Benoit Loppinet[b] and George Petekidis

Content:

1) Clay dispersion and emulsion preparation

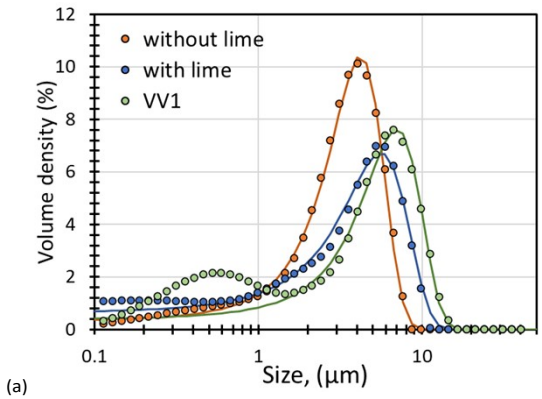

(a)

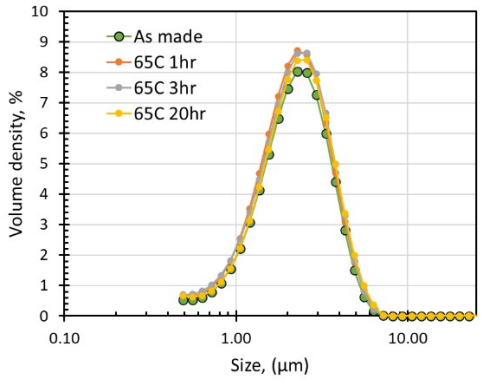

(b)

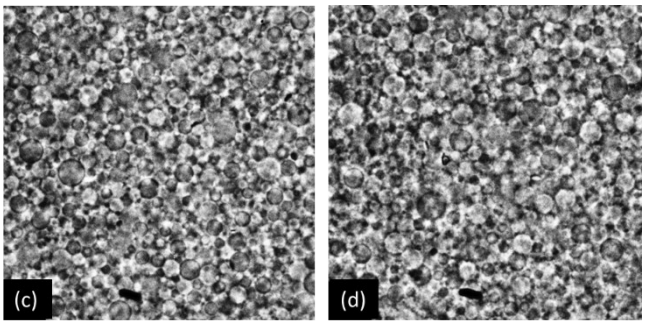

Figure S1: (a) Emulsion drop size distribution measured using a Mastersizer. Primary peaks have been fitted with a simple gaussian. (b) Separate preparation of VV1, measured after incubating at 65C for various periods. (c) VV1 imaged at 60 °C and (d) VV1 imaged after cooling to 20 °C.

Clay Dispersion: 200.0 g Clairsol 370 was put into a small metal cup and 4.60 g VG69 added over a few minutes with stirring. Sheared on Silverson (L4RT) mixer fitted with a square hole high shear screen at 6000 rpm for 12 minutes – final temperature ~ 55 °C. 0.20 g deionised water added, then mixture sheared again at 6000 rpm, using a cooling bath initially, then removing it about half-way through the time – final temperature 50 °C.

Emulsion: General lab oil-based drilling fluid preparation[1] follows a similar sequence. Using a high-shear Silverson mixer (L4RT) fitted with a square hole high shear screen at 6000 rpm, for each mixing step; (1) add the surfactant(s) to the oil and mix for 5 mins. (2) Add the clay and mix for 5 mins. (3) Add the lime and mix. (4) Add the brine and mix for 10 mins. Subsequently other additives and finally the barite are mixed. For VV1 we stop after step 4 and for the emulsion only we miss step (2). In all cases a heat treatment, under pressure at 120 °C for 16Hrs (Ofite™ aging cell) is the final step.

The emulsion drops are a few microns in diameter with a distribution as shown in figure S1a. The data are fitted with a simple Gaussian peak to give mean drop diameters and PDI's of: (i) emulsion without lime, 4.2µm, PDI=0.14; (ii) emulsion with lime, 5.6 µm, PDI=0.21; (iii) VV1, 7.0 µm, PDI=0.17. Although the same procedure is followed, we would expect and indeed see some batch-to-batch variation of drop size. Note that the lower peak in VV1 is likely associated with clays; its shape and position is quite variable in this measurement. In figure S1b are shown sequential measurements of VV1 without clay (i.e. emulsion) after incubating at 65 °C for various periods. The sample was placed in an oven in an enclosed container and aliquots taken at sequential times thereafter. The aliquots' size distributions were measured after cooling at 25 °C using a Mastersizer 3000. In figure S1c and d are shown microscope images of VV1 at 60 °C and 20 °C respectively.

The flow curves of the emulsion without clay, with and without lime, are shown in figure S2. The drop of the stress (or apparent viscosity plateau) at low shear rates is indicative of slip.

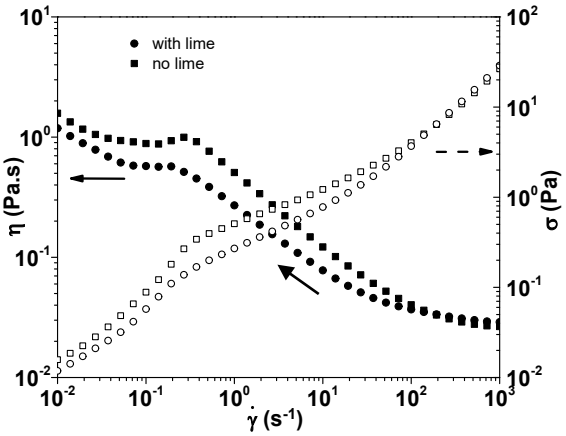

Figure S2: Flow curves, measured from high to low shear rates, for the brine emulsion in Clairisol 370 at 25 °C. Above 0.3 s^{-1} high-to-low and low-to-high curves overlay i.e. no hysteresis was observed. Lime is expected to activate the surfactant package and is always in excess in drilling fluids to control H_2S production. Viscosity versus shear rate (left) and stress versus shear rate (right).

2) Scattering length l* versus temperature for VV1

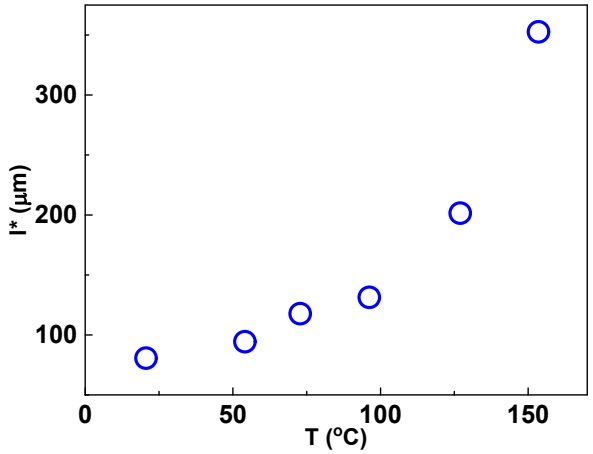

Figure S3: Evolution of the scattering length l* with temperature

3) DWS MSD spectra of VV1 aging at 25°C and 65 °C, including fast dynamics

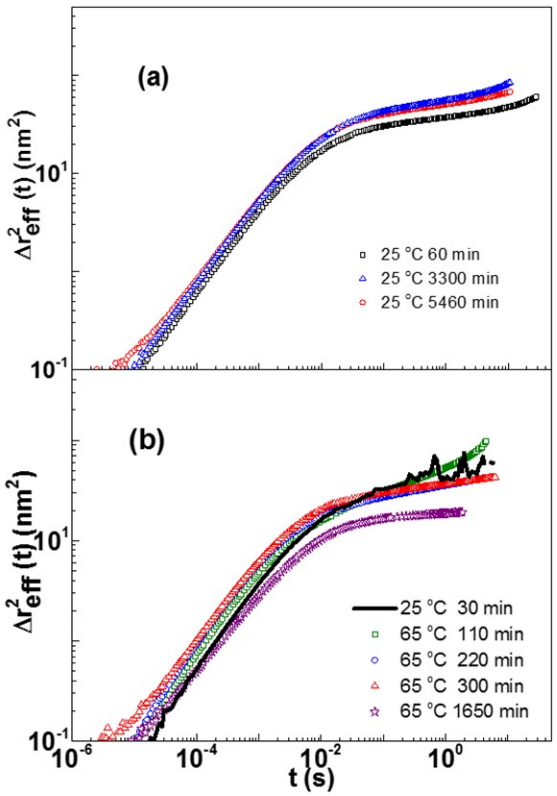

Figure S4: Correlation functions from VV1 (FORTH batch) at two different temperatures (T = 25 °C, top and T=65 °C, bottom) as a function of waiting time.

Aging measured in the second batch of VV1 (FORTH, Crete) at T=25 °C and T=65 °C, indicates a weaker slowing down of the slow mode at room temperature as compared to high (T= 65 °C) temperatures. The MSDs (in a.u.) as deduced from the DWS correlation functions are shown in figure S4. In qualitative agreement with the measurements presented in figure 6 a progressive increase of the non-ergodic plateau with waiting time is found which is stronger at high temperatures (65 °C) than at room temperature.

4) DWS MSD for emulsion with no clay : P,T dependence

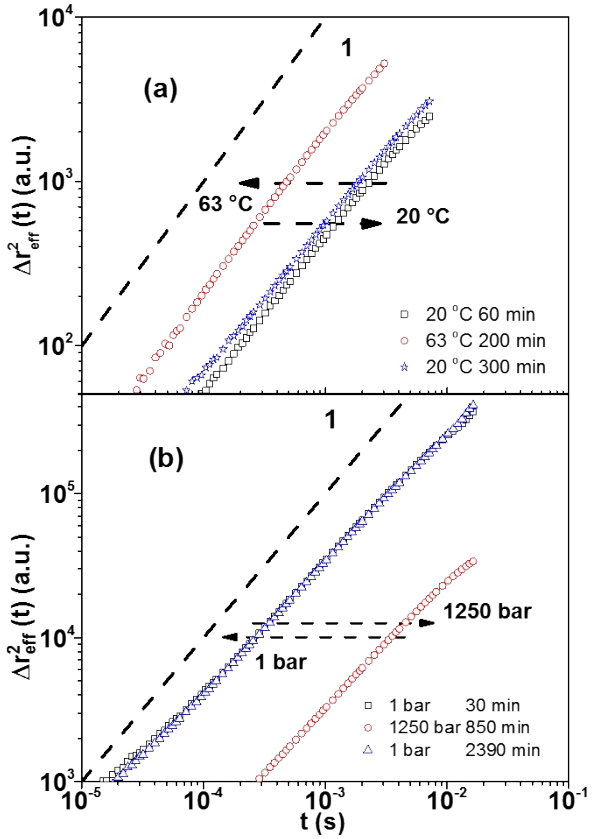

Figure S5: DWS MSDs in arbitrary units (a.u.) for the pure emulsion sample under (a) a temperature and (b) a HHP cycle. Dashed line indicate a typical diffusive MSD. The observed variation of the diffusion with P and T probably relates to variation of the oil viscosity.

The microscopic dynamics (MSD) of the emulsion droplets in the emulsion sample without clay followed by DWS during a temperature and pressure increase-decrease cycle are shown in figure S5.

5) Long time aging of VV1 at 100 °C: DWS, MSD and analysis

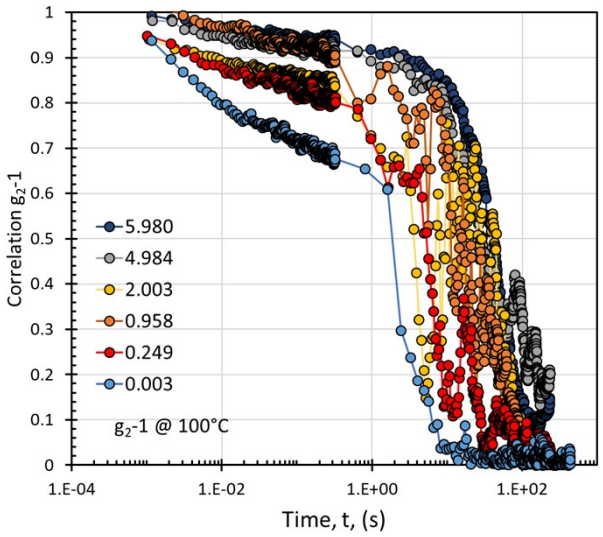

Figure S6: VV1 correlation functions as a function of extended waiting time at a temperature of 100 °C and pressure of 8.5 bar. Legend indicates waiting time in days. The first curve has a wait time of 254 s.

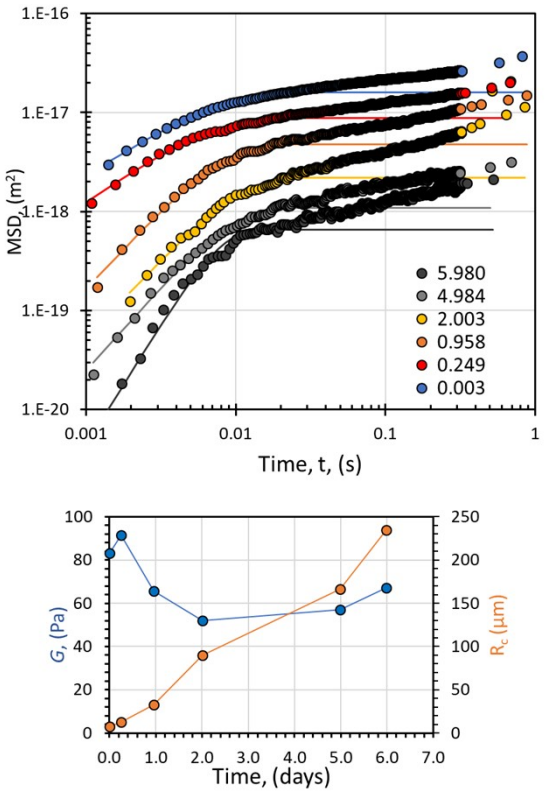

Figure S7 (a) VV1 MSD derived from data in figure S6 using equation (3). The legend indicates waiting time in days. (b) VV1 modulus and cluster size derived from the MSD in (a) using equations (6) and (7).

A VV1 sample (first batch) was held at 100 °C for six days and the correlation function monitored periodically. Data are shown in figure S6. Initially the sample exhibits a clear two relaxation spectrum i.e. a fast relaxation followed by a non-ergodic plateau that is eventually leading to a slower relaxation. As time progresses the longer relaxation becomes exceedingly noisy. The time for this onset (approximately 6 hours) corresponds to the onset of gel collapse and intermittency seen for this system[2]. Note that the DWS beam probes roughly halfway up the fluid column thus is not probing supernatant or sediment. At long times the spectrum again becomes steady but the plateau level has increased commensurate with a stronger confinement of the scatters. In Figure S7a we show the MSDs deduced from the correlation functions of figure S6. The progression of the curves in figure S7a clearly show an increasing confinement of the scattering entities as time progresses. These data are fitted using equation (6). The modulus and cluster size derived using equations (7) and (8) are then plotted as a function of sample age in figure S7b.

6) DWS spectra following high pressure application and release in VV1

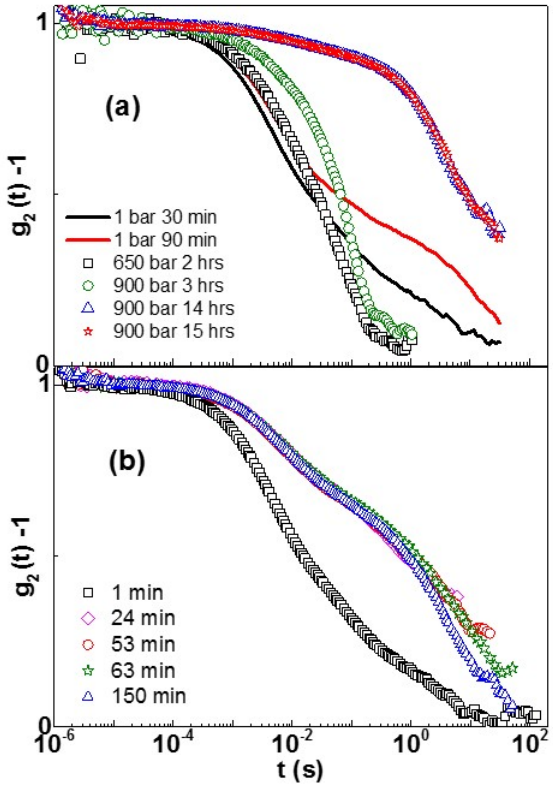

Figure S8: (a) DWS correlation functions following HHP application; series order: 1-2 at 1 bar (30-90 min); 3 at 650bar (120min); 4 reaching 900 bar (130min); at 900 bar (14-15 h) (on top of each other). (b) DWS correlation functions of VV1 following HHP release (0.9 kbar to 10 bar) after 15h at 0.9kbar); Indicated time is time after reaching 10 bar pressure.

An additional series of HHP cycle experiments with the full VV1 sample was performed in transmission under DWS conditions with a single coherence area detection set-up (PMT) which does not ensure a priori a proper ensemble average from a non-ergodic sample. However, the use of the Pusey- van Megen normalization method allows the calculation of the ensemble average correlation function as shown in Figure S8.

At the highest pressure, the two modes in the correlation function are barely discernable while upon reducing the applied pressure, the correlation function exhibits one main slow mode. As pressure is reduced further, the slow mode becomes faster, but the second slow mode does not reappear. Moreover, at 1bar the remaining dominant mode of the correlation function exhibits a similar relaxation process with the initial fast mode, before the HHP cycle.

Finally, upon following the time evolution of the correlation function after returning to ambient pressure from the HHP cycle the single, remaining, mode of the correlation function exhibits a progressive slow down with time (Figure S8).

1. API, *API/ISO standard*, 2016, **API 13I / ISO10416:2008**.
2. A. Clarke, L. Bailey and E. Jamie, presented in part at the AADE Fluids 2020, 2020.